Supplement of The Cryosphere, 19, 3309–3327, 2025
https://doi.org/10.5194/tc-19-3309-2025-supplement

The Cryosphere Open Access EGU

Supplement of

Improved modelling of mountain snowpacks with spatially distributed precipitation bias correction derived from historical reanalysis

Manon von Kaenel and Steven A. Margulis

Correspondence to: Manon von Kaenel (mvonkaenel@g.ucla.edu)

Contents of this file

Texts S1, S2, S3

Figures S1, S2, S3, S4, S5, S6, S7, S8

S1: Modelling approach

The reanalysis methodology applied in this study follows the approach described in Fang et al. (2022). In summary: the land surface model (LSM) used is the spatially-distributed SSiB–SAST model (Sun and Xue, 2001) which simulates a three-layer snowpack when snow depth exceeds 5 cm, and a one-layer scheme for shallower snow. This model integrates snow depth, snow density, and snowmelt, with mass balance components of rainfall and evaporation. It uses the BATS snow albedo model and the Liston Snow Depletion Curve (SDC; Liston 2004) to predict snow-covered areas.

The meteorological inputs include hourly 2-m air temperature, 2-m specific humidity, 10-m zonal and meridional wind speed, surface pressure, surface precipitation, and surface downwelling shortwave from MERRA2. These gridded fields are downscaled from the coarse resolution of 0.5° latitude by 0.625° longitude (~50 km) to the finer model resolution of 15 arcseconds (~500m) using bilinear interpolation and topographic corrections described in Girotto et al. (2014). The topographic corrections include the application of a lapse rate to the temperature field. The input meteorological data are subjected to perturbations to account for biases and uncertainties as follows:

- Precipitation: A lognormal distribution of factors with a mean of 1.80 and a coefficient of variation (CV) of 0.69 (Liu and Margulis, 2019).
- Air Temperature: Normally distributed additive error with a mean of +0.85 K (Girotto et al., 2014).
- Dew Point Temperature: Normally distributed additive error with a mean of −1.37 K (Girotto et al., 2014).
- Shortwave Radiation: Normally distributed multiplicative error with a varying correction factor based on the solar index (SI) (Girotto et al., 2014).

Other land surface model inputs include:

- topographic data from the 30-m Shuttle Radar Topography Mission (SRTM), with gaps filled by the Advanced Spaceborne Thermal Emission and Reflection (ASTER) version 2
- landcover data from the 1-km Advanced Very High Resolution Radiometer (AVHRR) product
- forest cover fraction data from the 30-m Global Land Cover Facility product, specifically the updated Landsat Tree Canopy Version 4.

All inputs are downscaled or aggregated to the model resolution.

References

Fang, Y., Liu, Y., and Margulis, S. A.: A western United States snow reanalysis dataset over the Landsat era from water years 1985 to 2021, Scientific Data, 9(1), 677, https://doi.org/10.1038/s41597-022-01768-7, 2022.

Girotto, M., Margulis, S. A., and Durand, M.: Probabilistic SWE reanalysis as a generalization of deterministic SWE reconstruction techniques, Hydrological Processes, 28(12), 3875-3895, https://doi.org/10.1002/hyp.9887, 2014.

Liston, G. E.: Representing Subgrid Snow Cover Heterogeneities in Regional and Global Models, Journal of Climate, 17(6), 1381-1397, https://doi.org/10.1175/1520-0442(2004)017<1381>2.0.CO;2, 2004.

Liu, Y. and Margulis, S. A.: Deriving Bias and Uncertainty in MERRA-2 Snowfall Precipitation Over High Mountain Asia, Frontiers in Earth Science, 7, https://doi.org/10.3389/feart.2019.00280, 2019.

Sun, S. and Xue, Y.: Implementing a new snow scheme in the Simplified Simple Biosphere Model, Advances in Atmospheric Sciences, 18(3), 335-354, https://doi.org/10.1007/BF02919314, 2001.

S2: Assimilation window for fSCA assimilation

The time window for fSCA assimilation is from the snow onset date to 1 April. The snow onset date is defined for each pixel-year as the first day when 3 consecutive days have maximum snow cover; we use this date to exclude fSCA observations that occur during early season snow accumulation events. We find that, without later ablation-season fSCA observations to correct the prior SWE estimates, these early-season fSCA observations tend to add more noise than value to the reanalysis. So, the assimilation window generally includes the period of time when the pixel is fully snow-covered, which may include some dips in snow cover relating to winter melt events as exemplified on days 40-50 in Fig. 3b and some portion of the ablation season depending on whether ablation happens before 1 April at that pixel.

S3: Streamflow observations

A daily time series of streamflow observations at the TGC (Tuolumne River at Grand Canyon) gage was constructed from records downloaded from the CDEC (California Data Exchange Center) platform. 15-min data was available for water years (WYs) 2009-2021, and daily data was available for WYs 2015-2021. In an effort to optimize data availability, we filled gaps in the 15-min data less than 3 hours long with linear interpolation, and aggregated it to a daily time step. From this constructed daily time series, we filled gaps less than 5 days long with a spline interpolation (for example, in mid-April 2021 in Fig. S1). Any remaining gaps in the daily constructed time series were filled with available daily data from CDEC. We

found that the constructed daily time series from 15-min data matched the daily data from CDEC exactly on overlapping days (for example, WY 2021 in Fig. S1). These steps yielded a complete daily time series of streamflow observations for April-July in WYs 2009-2021, except for WY 2019 when several weeks of data in April are still missing (Fig. S2).

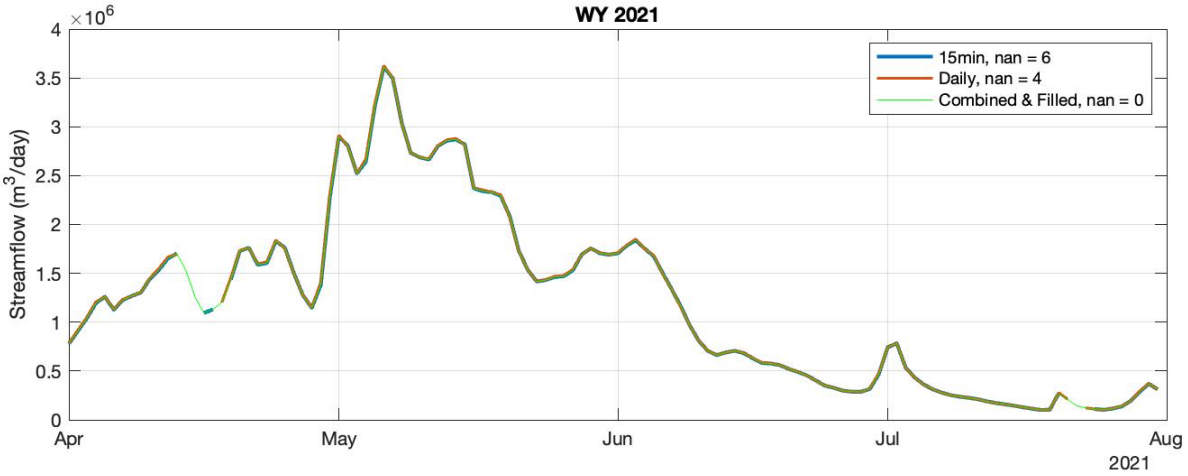

Figure S1. Time series of streamflow observations at the TGC gauge for April-July 2021. The blue line tracks the daily-aggregated 15-min data; the orange line tracks the daily data downloaded from CDEC; and the green line tracks the post-processed gap-filled time series.

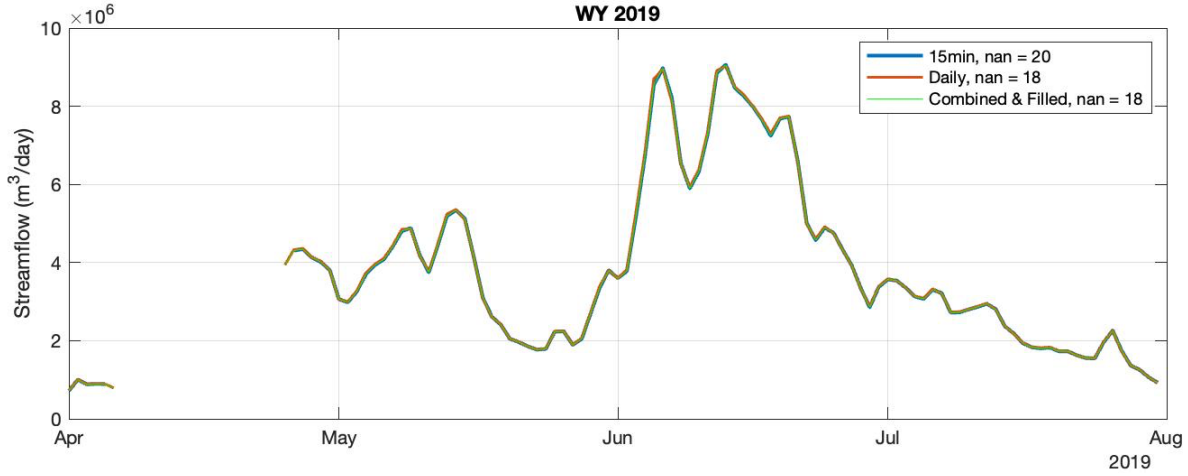

Figure S2. Time series of streamflow observations at the TGC gauge for April-July 2019. The blue line tracks the daily-aggregated 15-min data; the orange line tracks the daily data downloaded from CDEC; and the green line tracks the post-processed gap-filled time series.

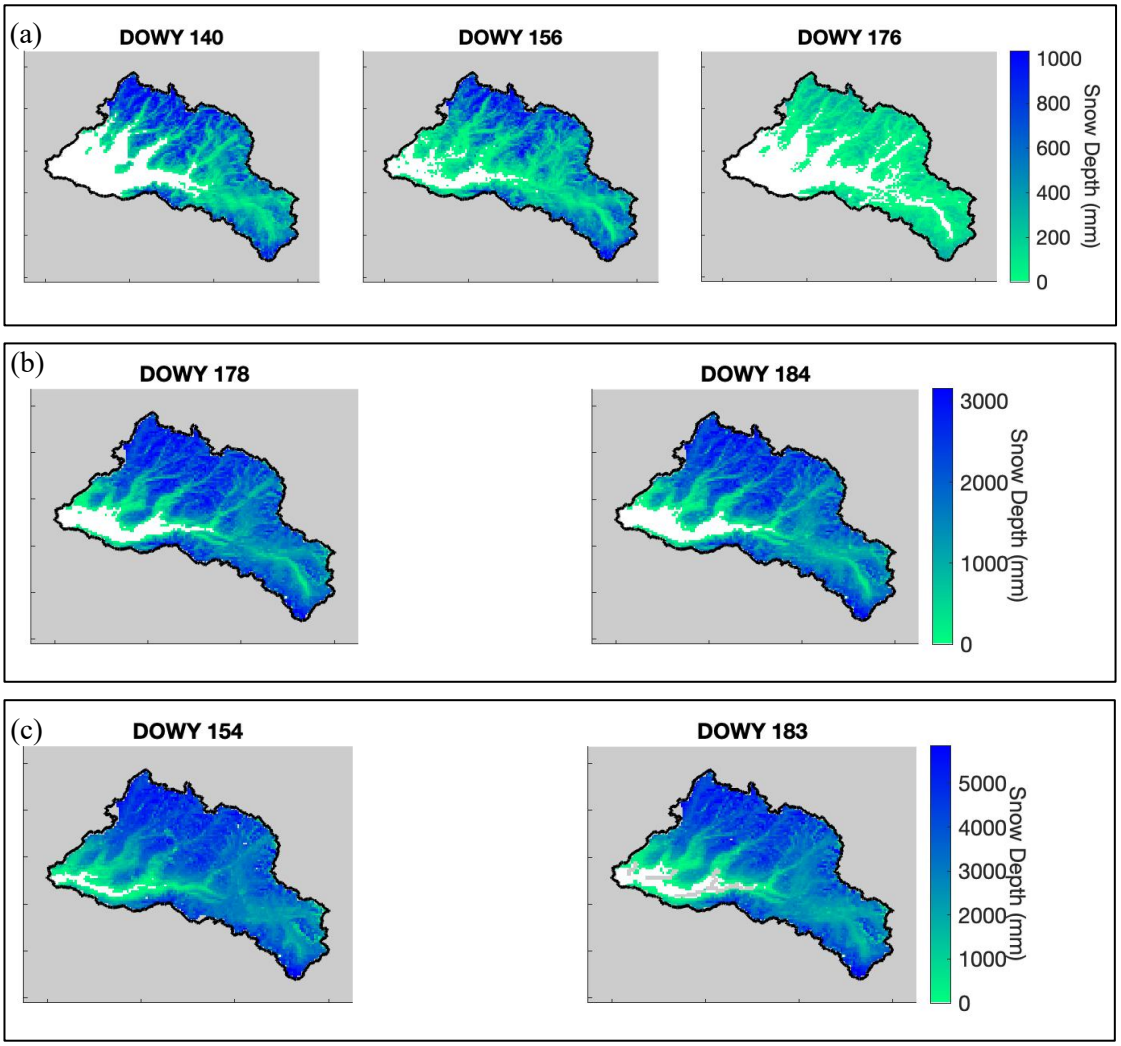

Figure S3. Maps showing the ASO-derived snow depth measurements over the Hetch Hetchy watershed used in data assimilation for (a) 2015, (b) 2016, and (c) 2017.

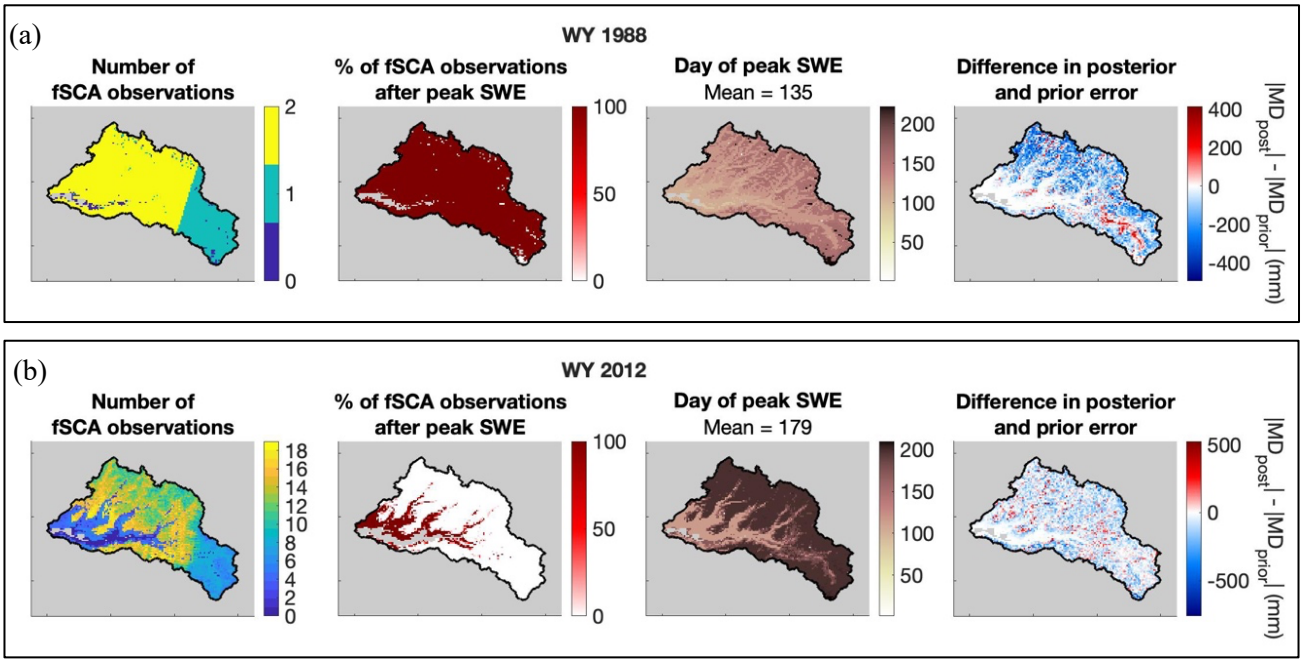

Figure S4. For the Case B + fSCA experiment, these maps illustrate (left to right) the number of assimilated fSCA observations; the percent of those fSCA observations that occur after pixel-wise peak SWE; the day of peak SWE; and the difference in posterior and prior error (where error is defined as the absolute difference between the SWE estimate and the historical reference) (a) WY 1998 and (b) WY 2012. In the right-most map, pixels coloured in blue indicate a reduction in error with fSCA assimilation, and red indicates an increase in error. Note that the watershed-scale NRMSD was reduced with fSCA assimilation for both water years shown.

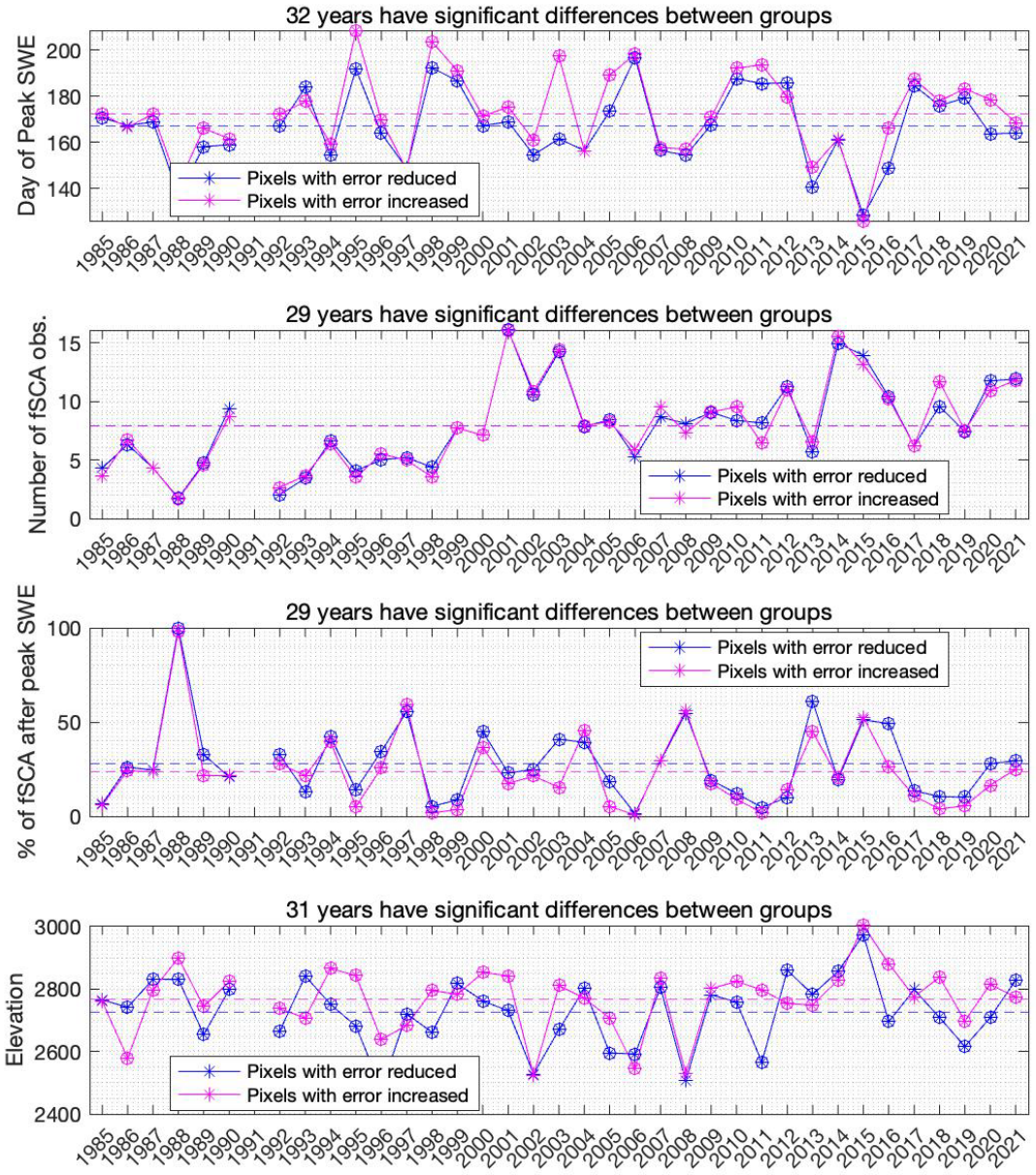

Figure S5. For the Case B + fSCA experiment, these time series track average values of 4 key metrics for model pixels with error reduced by fSCA assimilation versus pixels with error increased, where error is defined as the absolute difference with respect to reference 1 April SWE. A circle surrounds the yearly data point for years in which a statistically significance difference (p-value < 0.05 in a t-test) exists between the two groups of pixels. The dashed horizontal lines indicate the long-term average metric value for the two pixel groups. The metrics included are, from top to bottom: the day of peak SWE, the number of fSCA observations assimilated, the percent of those observations that occur after peak SWE, and elevation.

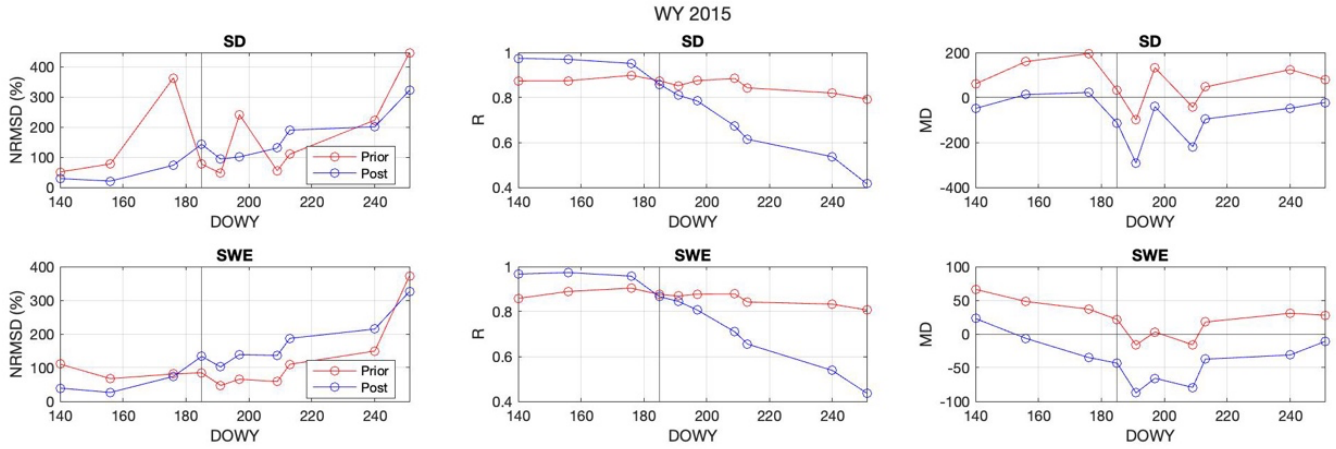

Figure S6. For WY 2015, a summary of the performance metrics (from left to right: NRMSD, R, and MD) for both prior (red) and posterior (blue) SWE and snow depth estimates in the Case B + SD experiment. Here, the reference is the ASO snow depth (top row) and ASO SWE (bottom row), and the metrics are evaluated on each day when ASO obtained measurements. The black vertical line indicates DOWY 185, the validation day for this year. The three prior ASO snow depth observations are assimilated into the posterior estimates in the Case B + SD experiment.

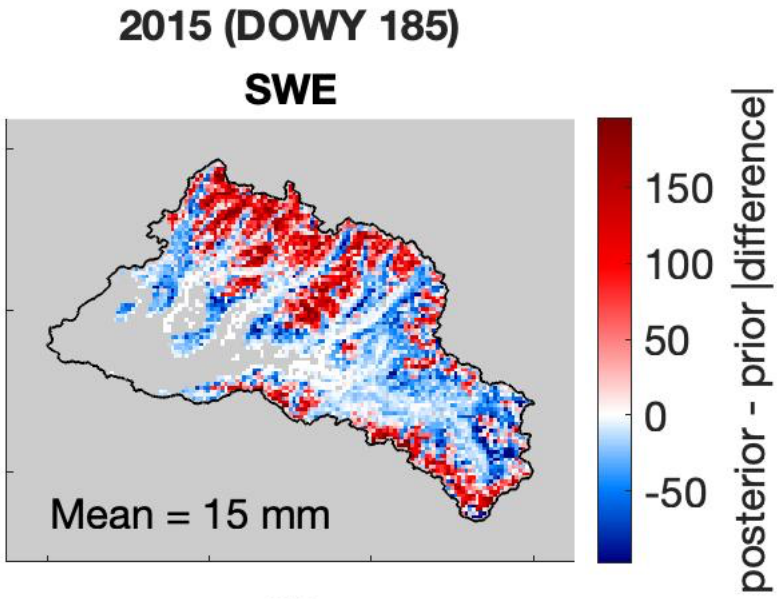

Figure S7. A map showing the change from the absolute difference relative to the ASO reference in prior SWE estimates to posterior SWE estimates for the Case B + SD experiment (|posterior – reference| – |prior – reference|), on WY 2015 DOWY 185. Areas in red indicate pixels where the posterior difference is greater than the prior difference. Note that pixels where both observed and simulated SWE is 0 are greyed out.

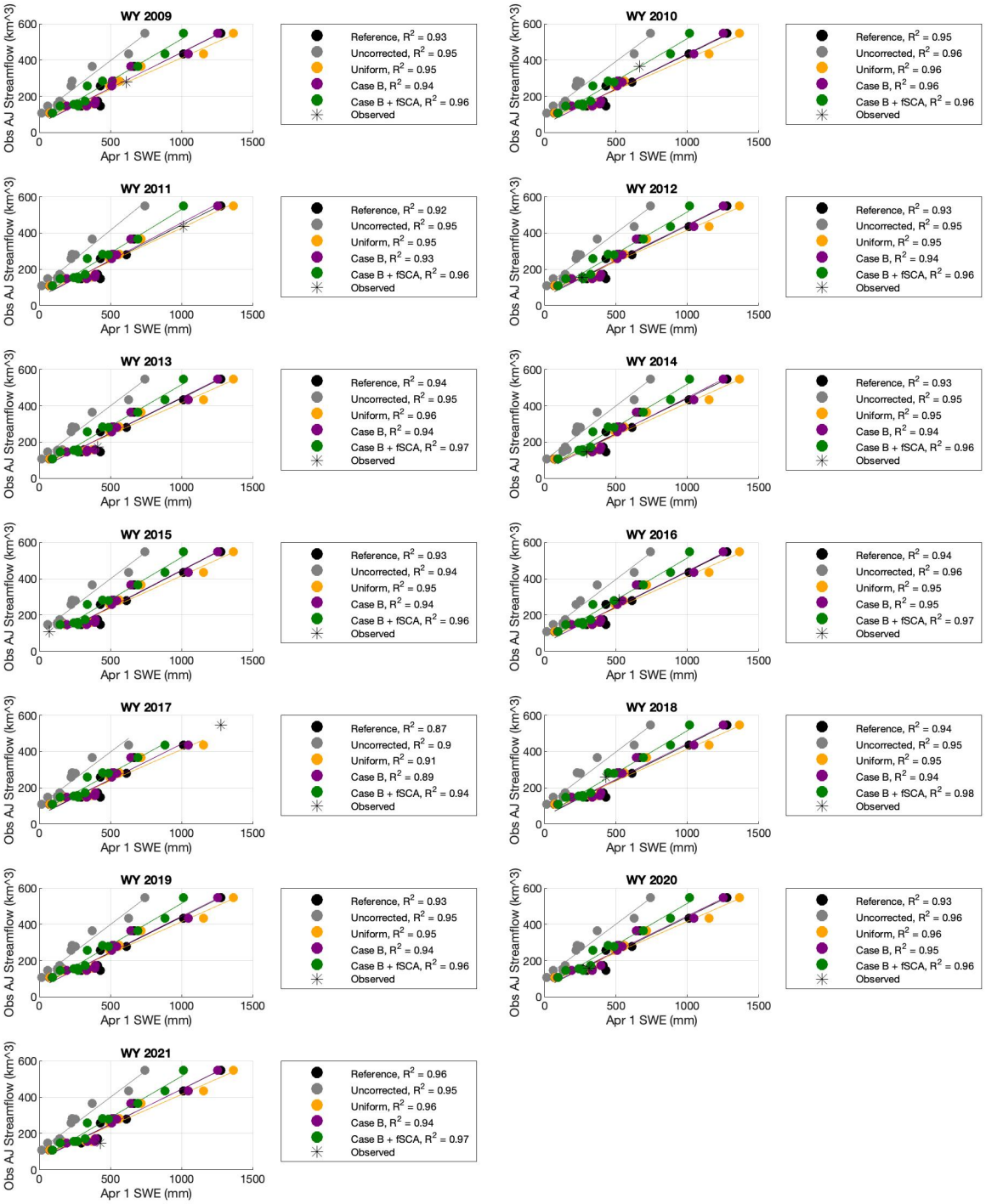

120 **Figure S8. For WY 2009-2021, scatter plots showing basin-averaged 1 April SWE from the historical reference and four experiments, and observed AJ streamflow volume. Each dot represents a different water year. Solid lines indicate the regression lines for that experiment. The R^2 for each linear regression is noted in the legend. Note that for a given year, that year's data is excluded from the regression. Instead, the reference 1 April SWE and observed AJ streamflow is plotted with a black asterisk symbol.**